

## ON LONG-TERM BEHAVIOR OF CABLES IN CABLE-STAYED BRIDGES

*By Yoshiji NIWA\**, *Hiroshi NAKAI\*\**, *Eiichi WATANABE\*\*\** and *Ikuo YAMADA\*\*\*\**

The Locked Coil Rope cables of cable-stayed bridges have reportedly undergone significant relaxation and the deflections of the girders have also increased noticeably year after year from a number of field measurements. In this paper, an attempt is made to account for such behavior analytically assuming that the cables follow the linear visco-elasticity law; whereas the girders and towers remain linearly elastic. Described herein are the determination of the visco-elastic constants, and numerical analyses performed on totally fifteen cable-stayed bridges by finite element method and the numerical Laplace inverse transformation; The results were compared with the measured data on two bridges.

### 1. INTRODUCTION

In recent years cable-stayed bridges seem to have been preferably constructed throughout the world. A cable-stayed bridge consists of three major elements: that is, girders, towers and cables. It is advantageous because of i) economical design through the pretensioning of cables, ii) easier erection using cables and iii) relatively simple and elegant alignment.

However, the Locked Coil Rope (hereafter referred to as LCR) cables have been reported to have undergone significant creep or relaxation. For this reason, DIN 1073 of West Germany requires that the creep strain from 0.010 % to 0.015 % must be taken into account in the design unless appropriate creep tests are conducted<sup>1)</sup>. In Onomichi Bridge<sup>2)</sup> (hereafter referred to as O Bridge) it was reported from a series of field measurements that creep strain of 0.018 % have occurred. On the other hand, in Kawasaki Bridge<sup>3,4)</sup> (hereafter referred to as KS Bridge), the maximum relaxation of the cables has been reported to have amounted to 11.8 % at 3.5 years after construction.

According to the study by Nakai et al.<sup>5)</sup>, the total creep elongation is the sum of the elongation of each component wire and the structural elongation caused by the relative movements between the interface of the wires; furthermore, they demonstrated that the creep elongation of the spiral ropes is several times larger than that of the wires themselves.

An attempt is made in this study to evaluate the creep and relaxation of cable-stayed bridges assuming that the cables follow the linear visco-elastic law based on the field measurements on the existing bridges

---

\* Member of JSCE, Dr. Eng., Professor, Department of Civil Engineering, Kyoto University (Sakyo-ku, Kyoto)

\*\* Member of JSCE, Dr. Eng., Professor, Department of Civil Engineering, Osaka City University (Sumiyoshi-ku, Osaka)

\*\*\* Member of JSCE, Ph. D., Dr. Eng., Associate Professor, Department of Civil Engineering, Kyoto University

\*\*\*\* Member of JSCE, M. S., Engineer, Honshu-Shikoku Bridge Authority (Minato-ku, Tokyo)

conducted by two different organizations.

## 2. CABLE-STAYED BRIDGES IN JAPAN

### (1) Cables<sup>6),7)</sup>

The types of cables can be classified into : LCR and Parallel Wire Strand (hereafter referred to as PWS). In case of the former in particular, a special attention is called for the creep phenomenon. Several characteristics of cables are investigated on 14 typical cable-stayed bridges in Japan and are listed in Table 1, together with KS Bridge, that is subjected to rather extensive study. Among those 15 bridges, PWS are used in 9 bridges and LCR in other 6 bridges. In Japan, LCR was used earlier, then PWS has become more popular. Recently, however, LCR tends to be in use again because of easiness to use and of the resistance against the corrosion. The maximum cable forces resulting from the combination of the live loads amount approximately to 10 % to 40 % of the breaking strength, and the prestress forces 1 % to 10 %.

### (2) Relative Stiffness Ratio of Cables

The design of cable-stayed bridges may be significantly controlled by the stiffness of cables. For simple representation of the load distribution to the main girder, tower and cables, the following ratio will be defined as the relative stiffness ratio of the cables :

$$\gamma = \frac{E_c \sum_i \frac{A_{ci}}{l_i} \sin^2 \theta_i}{E_c I_G / L_T^3} \dots \dots \dots (1)$$

where  $l_i$  : length of each cable,

$A_{ci}$  : area of each cable,

Table 1 Cable Dimensions of Cable-stayed Bridges in Japan.

No	Initial (Name)	Type of Cable Arrange	No. of Cable Planes	Ropes	Area $A_c$ (cm <sup>2</sup> )	Breaking Strength $\sigma_b$ (t/cm <sup>2</sup> )	Maximum Force $T_{max}$ (t)	Prestress Force $T_p$ (t)	$T_{max} / \sigma_b A$	$T_p / \sigma_b A$	$\gamma$ (x10 <sup>3</sup> ) Eq. (1)
1	Y	HARP (1)	1	PWS217X19	809.6	16.0	4,408	201	0.340	0.016	17.44
				PWS169X19	630.5	16.0	3,203	148	0.318	0.015	
				PWS217X13	553.9	16.0	3,347	212	0.378	0.024	
				PWS217X13	553.9	16.0	3,052	222	0.344	0.025	
2	S.H	FAN (2)	1	PWS169X7	381.9	16.5	901		0.143		8.85
				PWS127X6	381.9	16.5	801		0.127		
								784		0.124	
								636		0.101	
5	K	FAN Multi Cable	1	PWS271X2	106.4	15.7	539	40	0.323	0.024	7.92
				PWS184X2	72.3	15.7	366	79	0.323	0.069	
				PWS114X2	44.3	15.7	227	35	0.323	0.049	
4	R	FAN (6)	2	PWS217X2	85.2	15.2	430	130	0.331	0.100	0.25
3	T	FAN (2)	1	PWS154X16	483.7	15.7	2,548	556	0.335	0.073	5.21
				PWS127X12	299.2	15.7	1,167	549	0.248	0.117	
6	O	RADIAL (2)	2	LCR-D70X4	138.8	11.8	330	7	0.202	0.047	16.13
				LCR-D66X4	122.4	12.1	327	69	0.221	0.047	
				LCR-D56X4	89.6	11.8	218	57	0.206	0.054	
				LCR-D54X4	83.2	12.0	222	24	0.222	0.024	
7	S.G	HARP (3)	1	PWS169X19	630.5	16.5	3,137	453	0.302	0.044	1.09
				PWS169X13	431.4	16.5	1,967	58	0.276	0.008	
				PWS169X7	381.9	16.5	1,736	362	0.276	0.057	
				PWS127X6							
8	D	FAN (2)	2	PWS127X12	299.2	16.0	919		0.192		1.15
				PWS127X9	224.4	16.0	622		0.173		
				PWS127X12	299.2	16.0	1,044		0.218		
				PWS127X9	224.4	16.0	513		0.143		
9	A	HARP (2)	1	PWS127X7	281.8	16.0	1,350	100	0.299	0.022	1.84
				PWS91X6	281.8	16.0	962	500	0.213	0.111	
10	I	FAN (2)	2	PWS127X4	99.7	16.0	174	93	0.111	0.059	7.05
11	E	RADIAL (6)	2	LCR-F100φ	70.4	12.0	288		0.317		2.06
				LCR-E92φ	58.4	11.8	224		0.324		
				LCR-E80φ	44.8	11.9	170		0.320		
				LCR-D70φ	34.7	11.7	119		0.293		
12	G	FAN (3)	2	LCR-E80φX4	179.2	13.0	992	204	0.426	0.086	4.80
				LCR-D70φX4	138.8	13.0	589		0.326		
				LCR-D60φX4	102.0	13.0	440		0.322		
13	M	FAN (2)	2	LCR-D58φX12	280.8	15.0	1,685	200	0.400	0.048	0.32
14	S.1	HARP (2)	2	LCR-H100φX4	290.4	16.1	600	300	0.128	0.064	1.12
				LCR-E90φX4	228.8	13.4	270	175	0.088	0.057	
15	K.S	FAN	2	LCR-D50φ	18.2	11.4	33	26	0.158	0.127	0.17
				LCR-D70φ	33.8	12.0	94	35	0.233	0.086	

- $\theta_i$  : slope of each cable,
- $E_c$  : Young's modulus of cables,
- $E_G$  : Young's modulus of main girder,
- $I_G$  : moment of inertia of main girder,
- $L_T$  : total length of bridge.

The relationship between the total span length and the relative stiffness ratio with respect to the bridges considered in the proposed study is shown in Fig. 1.

### 3. FIELD MEASUREMENTS

#### (1) Scope

For the present, available field data are extremely limited on the long-term behavior of the cable-stayed bridges. Namely, only two sets of data are available for use. Those are on i) O Bridge and ii) KS Bridge. They consist of the time-dependent changes of the vertical deflections of the main girders and the cable tensions.

#### (2) KS Bridge<sup>3),4)</sup>

KS Bridge shown in Fig. 2 is a cable-stayed bridge of multi-cable type, over the Ohkawa River in Osaka for pedestrians and bicycles and was completed in 1978. It has two continuous spans of 87.5 m+40.65 m, and has 20 LCR cables. Table 2 shows the dimensions of the cables. For detailed descriptions on the actual erection of cables, the readers are recommended to see reference 3).

The cable forces were measured two times so far, namely, on completion and three years and a half after that by the free vibration method using accelerometers and spectrum analyzer by Osaka Municipal Office and Kurimoto Steelwork<sup>4)</sup>. Some of the authors were fortunate enough to participate the last measurement through the courtesy of Osaka Municipal Office.

The camber has been measured three times : on completion, one year and a half afterward, and three years and a half afterwards, respectively.

#### (3) O Bridge<sup>2)</sup>

O bridge has three continuous spans and the center span is 215 m. The cable alignment is of radial type

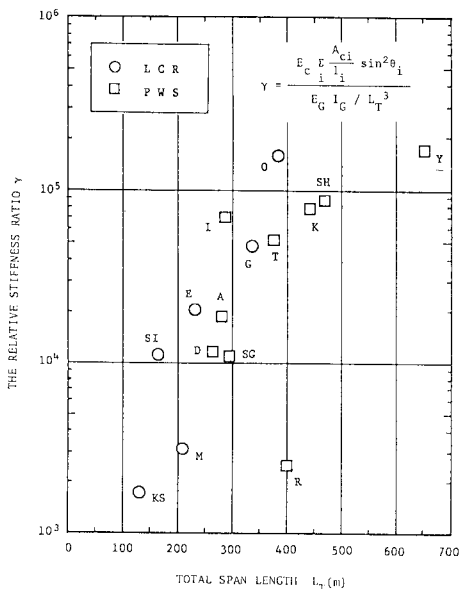


Fig. 1 Relationship between Total Span Length and the Relative Stiffness Ratio.

and 8 cables are connected at each stream side of the main girder. Each cable consists of 4 LCRs. The field measurements were performed 8 times on the vertical deflections of the main girder. They were found to be significantly large even at the first field measurement and were finally decided to be retightened after 8 years from the completion. For detailed descriptions on the fabrication and erection of cables, the readers are recommended to see references 8) and 9).

The bridge dimensions and the results at the completion, 4 and 8 years after the completion are shown respectively in Fig. 3. After 8 years from the completion, the deflection at the center span amounted

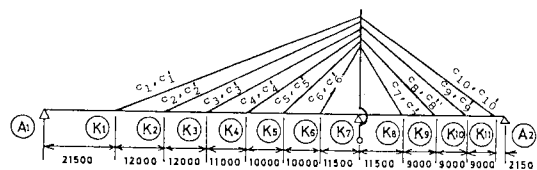


Fig. 2 KS Bridge.

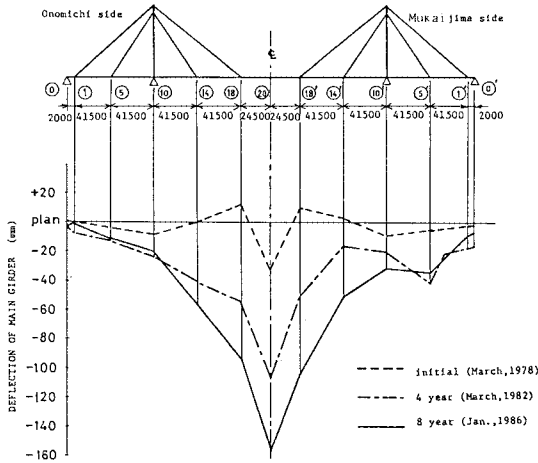


Fig. 3 Measured Deflection of O Bridge.

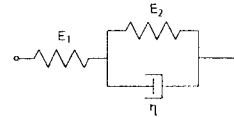


Fig. 4 Three-Element Model.

to 158 mm below the original configuration.

#### 4. METHOD OF ANALYSIS

##### (1) Linear Visco-Elastic Model of Cables

The linear visco-elastic model is adopted for convenience to the cables. From the fact that the maximum cable stresses do not amount to more than 30 % of the breaking stresses of the cables, it may be quite reasonable to assume that the creep may remain in the stage of the initial creep.

The linear visco-elasticity is defined by Boltzmann in 1-dimensional problem as follows<sup>(10), (11)</sup> :

$$\sigma(t) = \int_{-\infty}^t G(t-\tau) \frac{\partial e(\tau)}{\partial \tau} d\tau$$

$$e(t) = \int_{-\infty}^t J(t-\tau) \frac{\partial \sigma(\tau)}{\partial \tau} d\tau \quad \dots \dots \dots (2)$$

Thus, the relationship between the stress and strain, that is, the constitutive equation can be expressed in terms of the convolution. Consequently, the governing equations derived from this can be shown to take the form of Volterra's linear integral equation of the first kind. Furthermore, Volterra's principle states that any problem of the theory of hereditary elasticity can be solved in exactly the same way as the corresponding problem in the normal theory of elasticity except that in the final result the elastic constants must be replaced by elastic operators. As a matter of fact, using Laplace transform, and letting  $\bar{f}(s)$  designate the Laplace transform of a function  $f(t)$ , then it is quite easy to show that Eq. (2) can be transformed into :

$$\bar{\sigma}(s) = \bar{E}(s) \bar{e}(s) \quad \dots \dots \dots (3)$$

where  $\bar{E}(s) = s\bar{G}(s)$

in which  $\bar{G}(s)$  and  $\bar{E}(s)$  is referred to as the relaxation function and the Young's modulus in the Laplace image space  $s$ , respectively.

The three-element model adopted in this study, slightly different from what is called "standard solid model" by Sonoda et al.<sup>(12)</sup>, is shown in Fig. 4. :

It consists of elastic springs  $E_1$  and  $E_2$ , and a dash-pot with the viscosity constant  $\eta$ . The stress-strain relationship is given by :

$$\dot{\sigma} + \lambda\sigma = E(\dot{e} + \mu e) \quad \dots \dots \dots (4)$$

where

$$E = E_1$$

$$\begin{aligned} \lambda &= (E_1 + E_2) / \eta \dots\dots\dots (5) \\ \mu &= E_2 / \eta \end{aligned}$$

and the dot implies the differentiation with respect to the time  $t$ . Eq. (4) can be transformed into the following, upon Laplace transform assuming that  $\sigma(+0) = Ee(+0)$  :

$$\begin{aligned} \bar{\sigma}(s) &= E \frac{s + \mu}{s + \lambda} \bar{e}(s) \\ &= \bar{E}(s) \bar{e}(s) = s \bar{G}(s) \bar{e}(s) \dots\dots\dots (6) \end{aligned}$$

where

$$\bar{E}(s) = E \frac{s + \mu}{s + \lambda} \dots\dots\dots (7)$$

$$\bar{G}(s) = E \frac{s + \mu}{s(s + \lambda)} \dots\dots\dots (8)$$

In case strain  $e(t)$  is known, then, from Eq. (6) it yields :

$$\bar{\sigma}(s) = E \left( \bar{e}(s) - (\lambda - \mu) \frac{\bar{e}(s)}{s + \lambda} \right) \dots\dots\dots (9)$$

In the case of the relaxation problem, that is, when  $e(t) = e(0) = e_0 (t \geq 0)$ ,  $e(t) = 0, (t < 0)$ , it is easy to show that

$$\frac{\sigma(t)}{\sigma_0} = \frac{1}{1 + \rho} (\rho + \exp(-\lambda t)) \dots\dots\dots (10)$$

where

$$\rho = E_2 / E_1 \dots\dots\dots (11)$$

On the contrary, solving Eq. (6) for the strain, it can be seen that

$$\bar{e}(s) = \frac{1}{E} \left( \bar{\sigma}(s) + (\lambda - \mu) \frac{\bar{\sigma}(s)}{s + \lambda} \right) \dots\dots\dots (12)$$

In the case of the creep problem, that is when  $\sigma(t) = \sigma(0) = \sigma_0 (t \geq 0)$ ,  $\sigma(t) = 0, (t < 0)$ , it is also easy to show that

$$\frac{e(t)}{e_0} = \frac{1}{\rho} ((1 + \rho) - \exp(-\mu t)) \dots\dots\dots (13)$$

In actual cable-stayed bridges, cables are neither in the state of creep in a narrow sense of increasing strain on a constant stress, nor in the state of relaxation again in a narrow sense of decreasing stress on a constant strain, but it is reasonable to consider that both phenomena occur simultaneously.

The coefficient of the model may be determined from the creep test of ropes themselves. However, other factors such as the slip out of sockets or the deformation of bolts, and the settlement of the supports may affect the time-dependent behavior of cable-stayed bridges. Thus, it is difficult to determine the coefficients of the cable model solely from the creep tests of the component wires.

In the proposed study, thereby, the coefficients will be determined on the basis of the data obtained from the field measurements on the cable and the cambers of the main girders. The data of cable tension measurements through the vibration tests can be considered to be relatively reliable. The elongations of cables, nevertheless, can not be calculated correctly merely from the camber measurements because towers deform simultaneously. In view of the fact that no data is available with respect to the tower, an attempt is made to determine the constants of the cable making the best use of the existing data.

When the actual phenomenon can be regarded as a relaxation problem, Eq. (10) can be solved as follows :

$$\lambda = -\frac{1}{t} \ln \left( (1 + \rho) \frac{\sigma(t)}{\sigma_0} - \rho \right) \dots\dots\dots (14)$$

If the stresses  $\sigma(t_1), \sigma(t_2)$  are given at two different time stations  $t_1, t_2$  and if  $\lambda$  remains constant, then,

$$\frac{1}{t_1} \ln \left( (1 + \rho) \frac{\sigma(t_1)}{\sigma_0} - \rho \right) = \frac{1}{t_2} \ln \left( (1 + \rho) \frac{\sigma(t_2)}{\sigma_0} - \rho \right) \dots\dots\dots (15)$$

Thus,  $\lambda$  can be determined by letting  $\rho$  satisfy Eq. (15) and upon its substitution to Eq. (14).

On the other hand, when the actual phenomenon can be regarded as a creep problem Eq. (13) can be solved as

$$\mu = -\frac{1}{t} \ln \left( (1 + \rho) - \rho \frac{e(t)}{e_0} \right) \dots \dots \dots (16)$$

If the strains of the cable  $e(t_1)$ ,  $e(t_2)$  are given at two different time stations  $t_1$ ,  $t_2$  and if  $\mu$  remains constant, then,

$$\frac{1}{t_1} \ln \left( (1 + \rho) - \rho \frac{e(t_1)}{e_0} \right) = \frac{1}{t_2} \ln \left( (1 + \rho) - \rho \frac{e(t_2)}{e_0} \right) \dots \dots \dots (17)$$

Therefore,  $\mu$  can be determined by letting  $\rho$  satisfy Eq. (17) and upon its substitution to Eq. (16). Unfortunately, since the sufficient relaxation data are not accumulated in view of the fact that the cable tensions have been measured only once after the completion of the bridge, the determination of the cable constants merely from the vibration tests will be found impossible. Thus, an attempt is made to determine the constants from the camber measurements assuming that the problem is the creep problem using only the data of cables that did not undergo significant change of the cable force, and the results were compared with the results from the tension measurements.

### 5. FORMULATION FOR NUMERICAL CALCULATION

#### (1) Scope

The long-term behavior of the cable-stayed bridges can be analyzed by finite element method. From the Volterra's principle, the stiffness matrix of linear visco-elastic cables can be superimposed to that of the linear elastic girders and towers in the Laplace image space  $s$  to form the global equilibrium equation of cable-stayed bridge. After solving this equation the final solutions will be obtained in the real time domain through the numerical Laplace inverse transformation.

#### (2) Formulation by Finite Element Method

Since the girders and towers are linearly elastic, the stiffness matrix  $K_{ij}$  for a beam element is expressed as follows :

$$K_{ij} = \int_V B_{mi} E_{mn} B_{nj} dV \dots \dots \dots (18)$$

where  $B_{mi}$  or  $B_{nj}$ ,  $E_{mn}$ , and  $V$  designate the strain matrix, the elastic modulus matrix, and volume of the element, respectively.

As cables are assumed to be linearly visco-elastic, the stiffness matrix is given by :

$$\bar{K}_{ij}(s) = \int_V B_{mi} \bar{E}_{mn}(s) B_{nj} dV \dots \dots \dots (19)$$

where  $\bar{E}_{mn}(s)$  designates the elastic modulus in the Laplace image space and is represented from Eq. (8) as follows :

$$\bar{E}_{mn}(s) = \bar{E}(s) = E \frac{s + \mu}{s + \lambda} \dots \dots \dots (20)$$

Combining these stiffness matrices in the Laplace image space,  $s$ , the equilibrium equation of the total bridge is given by

$$\begin{bmatrix} \bar{K}_{11}(s) & \bar{K}_{21}(s) \\ \bar{K}_{21}(s) & \bar{K}_{22}(s) \end{bmatrix} \begin{Bmatrix} \bar{w}_1(s) \\ \bar{w}_2(s) \end{Bmatrix} = \begin{Bmatrix} \bar{P}_1(s) \\ \bar{P}_2(s) \end{Bmatrix} \dots \dots \dots (21)$$

where  $K_{ij}$ ,  $W_i$ , and  $P_i$  refers to the stiffness matrix, the nodal displacement, and the nodal forces, respectively. Moreover, subscript 1, and 2 refers to the main girder and tower, respectively. In the proposed study, the forces consist of the dead load and the prestress force induced to the cables. The following equations hold for the complete system :

$$(\overline{K}'(s))\{\overline{w}(s)\}=\{\overline{P}'(s)\} \dots\dots\dots (22)$$

Similarly, for the system under erection :

$$(\overline{K}''(s))\{\overline{w}''(s)\}=\{\overline{P}''(s)\} \dots\dots\dots (23)$$

The total displacements and stresses can be obtained as the sum of each system by the principle of superposition. Consequently, the displacements of girders and towers are obtained in the image space :

$$\begin{aligned} \{\overline{w}(s)\} &= \{\overline{w}'(s)\} + \{\overline{w}''(s)\} \\ &= (\overline{K}'(s))^{-1} \{\overline{P}'(s)\} + (\overline{K}''(s))^{-1} \{\overline{P}''(s)\} \dots\dots\dots (24) \end{aligned}$$

( 3 ) Numerical Laplace Inverse Transformation

The obtained solutions, nevertheless, constitute sets of numerical data in the image space  $s$ , and not in the real time domain  $t$ . It becomes necessary to apply the Laplace inverse transformation to the solutions so that they correspond to the real time  $t^{(13)-(15)}$ .

For successful execution of the numerical Laplace inverse transform, several considerations will be necessary. Regarding the choice of the interval to be subjected to the inverse transform, Izumi has proposed the following method<sup>(6)</sup> : First, examine the variation of the Young's modulus in the image space  $s$ , and plot the value of  $\overline{E}(s)$ . Secondly, find the interval in which this value changes and use this interval for the inverse transformation for  $\overline{f}(s)$ . Finally, apply appropriate regression formula based on the least square procedure in the prescribed interval so that the solution satisfy the limit theorems.

At first, the nondimensionization will be performed on time. The Laplace transformation is defined as follows,

$$\overline{w}(s) = \int_0^\infty \exp(-st)w(t)dt \dots\dots\dots (25)$$

Let us non-dimensionalize the expression in terms of a parameter,  $T$  :

$$t = T\bar{t}, \quad s = \bar{s}/T \dots\dots\dots (26)$$

Substitution of Eq. (26) into Eq. (25) yields

$$\frac{\overline{w}(s)}{T} = \int_0^\infty \exp(-\bar{s}\bar{t})w(T\bar{t})d\bar{t} \dots\dots\dots (27)$$

The above equation shows that the Laplace transform of  $w(T\bar{t})$  on  $t$  becomes  $\overline{w}(s)/T$  and that the Laplace inverse transformation of  $\overline{w}(s)/T$  on  $s$  becomes  $w(T\bar{t})$ . The parameter  $T$  is selected to be  $\eta/E$ , which is usually referred to as the delay time.

In the proposed study the solution of creep and relaxation is approximated as the sum of exponential functions.

$$w(T\bar{t}) = \sum_i^N a_i \exp(-\bar{b}_i\bar{t}) \dots\dots\dots (28)$$

where  $\bar{b}_i = Tb_i, \quad b_1 = 0$

Then the square error  $f$  can be formulated as :

$$f = \frac{1}{2} \sum_{j=1}^k \left( \sum_{i=1}^N \frac{a_i}{\bar{s}_j + \bar{b}_i} - \frac{\overline{w}(s_j)}{T} \right)^2 \dots\dots\dots (29)$$

where  $k$  refers to the number of the terminal points in the Laplace space,  $s$ . The values of  $a_i$  and  $b_i$  must be so determined as to satisfy the limit theorems and minimize function  $f$ . Now, letting  $N=2$ ,  $a_i$  can be determined as :

$$a_1 = w_\infty, \quad a_2 = w_0 - w_\infty \dots\dots\dots (30)$$

Furthermore, from the condition that  $\frac{\partial f}{\partial \bar{b}_2} = 0$

$$\sum_{j=1}^k \left( \frac{a_1}{\bar{s}_j} + \frac{a_2}{\bar{s}_j + \bar{b}_2} - \frac{\overline{w}(s)}{T} \right) \frac{1}{(\bar{s}_j + \bar{b}_2)^2} = 0 \dots\dots\dots (31)$$

The value of  $\bar{b}_2$  which satisfies the above transcendental equation can be found through the Regula Falsi

Method.

6. NUMERICAL ILLUSTRATIONS<sup>17)</sup>

(1) KS Bridge

The relative stiffness ratio is  $0.17 \times 10^4$ , which is much less than those for the other cable-stayed bridges.

Fig. 5 shows KS Bridge model and its model dimensions, respectively. KS Bridge was constructed in the following process, and the prestress was introduced by means of the jack-up and -down of the main girder. Thus, the analysis was made in conformity with the actual construction process :

- 1) Pre-dead Load : A temporary support is set up at point  $K_4$ , the bridge girder is assumed to be three-span continuous.
- 2) Jack Up : The girder is jacked up by 700 mm at point  $A_1$  ; by 100 mm at point  $K_4$  ; while the tower is set back by 100 mm at its top. The cables having the prescribed lengths are fastened to the main girder without initial stresses.
- 3) Remove Temporary Support : Temporary support at point  $K_4$  is removed.
- 4) Jack Down : The girder is jacked down by 700 mm at point  $A_1$ . Then, prestress forces are introduced into cables.
- 5) Post-Dead Load : The post-dead load is applied to the completed bridge.

The pre-dead load of steel girders is 1.682 t/m. The weights of cables vary from 0.344 t to 1.044 t, and the post-dead load is calculated to be 0.447 t/m. Furthermore, Young's modulus of girders and towers is  $E=2.1 \times 10^6$  kg/cm<sup>2</sup>, and that of cables is  $E_c=1.6 \times 10^6$  kg/cm<sup>2</sup>, respectively.

The coefficients,  $E_1$ ,  $E_2$ , and  $\eta$  of three-element model for cables are determined based on the measured data in the following manner : Firstly, a spring constant  $E_1$  is assumed to be the Young's modulus of cables,  $E_c$ . The vertical deflection of main girders was measured at 1.5 year and 3.5 years after the completion of the bridge. Then, the elongation and strain increments of cables are calculated from the measured data neglecting the set-back of towers. Visco-elastic constants are determined by Eq. (16) from the measured strains of cables obtained at different time stations with an appropriate modification made taking into account the settlement of the supports :  $\rho=5.0$ ,  $\mu=0.39$  ;  $E_2=8.0 \times 10^6$  kg/cm<sup>2</sup> and  $\eta=20.5 \times 10^6$  year kg/cm<sup>2</sup>.

Fig. 6 shows the relaxation of Cable 1 and Cable 10 ; whereas, Fig. 7 shows the creep deflection of the girder. Plotted also herein are the measured data. However, much discussions will be necessary with respect to whether the prediction of the future response is correct or not and how well it is considered to be fitted with measured data.

(2) O Bridge

The relative stiffness ratio is  $16.13 \times 10^4$ , which is comparatively larger than the other bridges. The

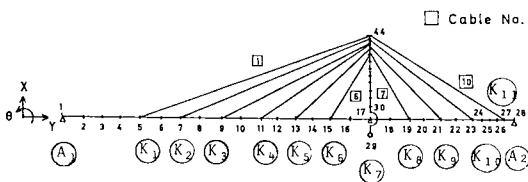


Fig.5 KS Bridge Model.

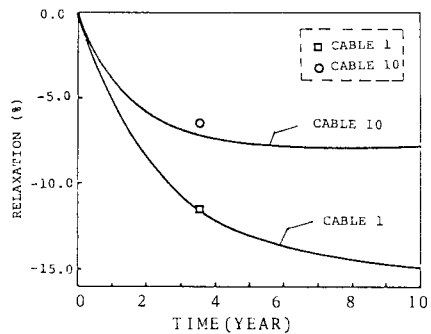


Fig.6 Relaxation of Cables 1 & 10.



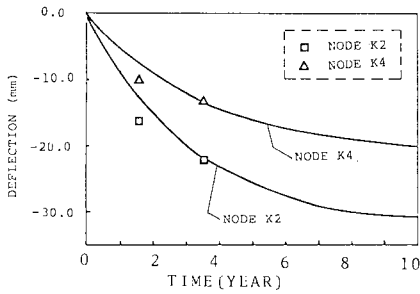


Fig. 7 Change of Deflection.

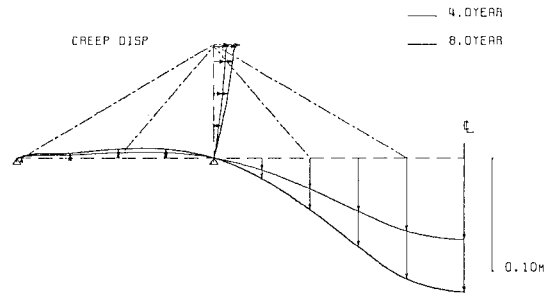


Fig. 9 Change of Deflection (O Bridge).

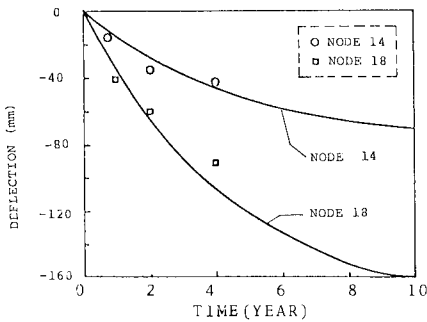


Fig. 8 Change of Deflection, Node 14 & 18, O Bridge.

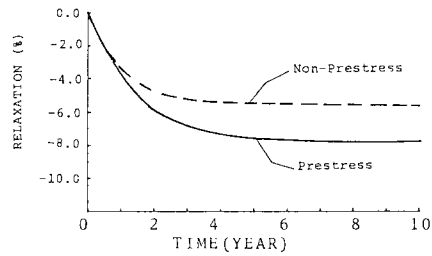


Fig. 10 Tension Change of Cable 10.

measurement of the deflection had been performed every one or two years after the completion.

Upon substitution of the cable strains at two different time stations of 4 years and 8 years after the completion into Eq. (17), the coefficients are determined as :  $\rho=2.0$ ,  $\mu_6=0.109$ ,  $E_1=E_c=1.6 \times 10^6$  kg/cm<sup>2</sup>,  $E_2=3.2 \times 10^6$  kg/cm<sup>2</sup> and  $\eta=29.5 \times 10^6$  year kg/cm<sup>2</sup>.

Fig. 8. shows the predicted change of the deflection at (14) and (18) plotted against the measured data taking into account only the dead load. The change of the deflection after 4 years and 8 years are illustrated in Fig. 9, respectively. Again, discussions may be made whether the prediction is good or not. However, from the available set of data, this may be as much as what can be predicted. Besides, it can be seen that the simple application of the principle of least squares without regard to the structural model may result in the better fit to the measured value.

## 7. EFFECTS OF PRESTRESS AND STIFFNESS RATIO

### (1) Effect of Prestress

Sometimes prestress is introduced to cables, either by using shim plates, by jack-up and-down of the main girder or the saddle of cable anchors, although the magnitude of prestress itself is not so large as seen from Table 1. This is mainly to improve the bending moment distribution of the main girder. To find the effect of this prestress, a comparative analysis was performed on KS Bridge in both cases of with and without the prestress.

The relaxation of Cable 10 is shown in Fig. 10. The relaxation in case of prestress is 7.8 % after 10 years, compared with 5.5 % in case of non-prestress. Shown also in Fig. 11. is the increment of deflection at Point K 2.

### (2) Effect of Relative Stiffness Ratio

Using the spring constant ratio :  $\sigma=E_1/E_2=2.0$  which is found to be fitted for O Bridge, the effect of the relative stiffness ratio is investigated.

Fig. 12 shows the relation between the relative stiffness ratio and the ultimate relaxation of cables

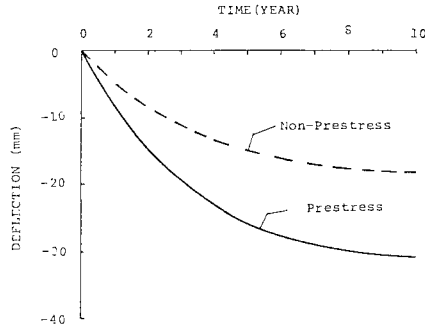


Fig.11 Increment of Deflection at  $K_2$ .

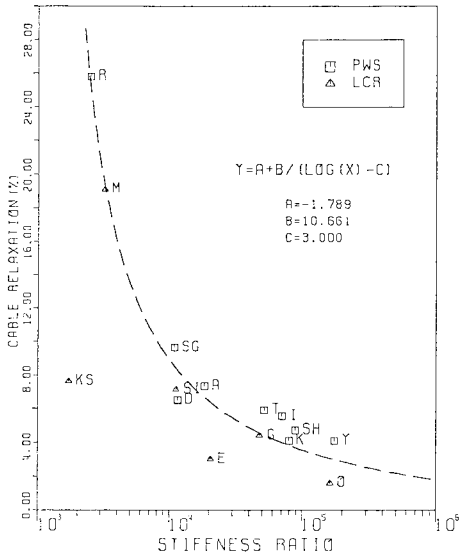


Fig.12 Relationship between Relative Stiffness Ratio and Relaxation.

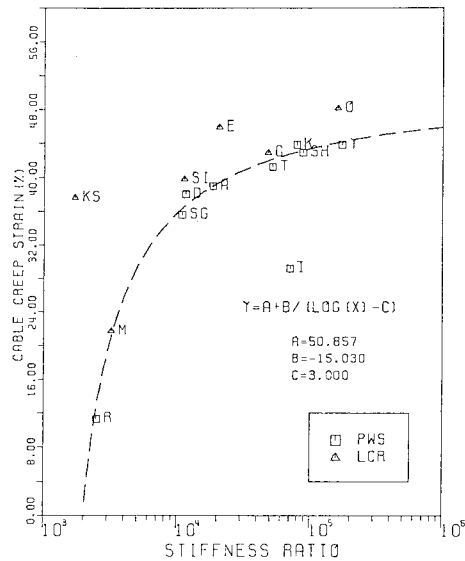


Fig.13 Relationship between Relative Stiffness ratio and Ratio of Creep Strain to Initial Strain.

considering only dead load. It may be obviously seen that the greater the relative stiffness ratio is, the less the relaxation of cables. The broken curve in this figure is a hyperbola obtained through the regression formula on the least square scheme.

Fig. 13 shows the relation of the relative stiffness ratio and the ratio of the ultimate creep strain to the initial strain. It may be observed that the greater the relative stiffness ratio is, the greater the ratio of creep strain becomes. Although Figs. 12 and 13 are obtained from very crude assumption of  $\rho=2.0$ , they may be used to know approximately how much creep and relaxation can be expected once the stiffness ratio is given.

### 8. CONCLUDING REMARKS

The conclusion obtained from the proposed study can be summarized as follows :

- (1) If changes of cables or cambers are measured at two independent time stations besides on the completion, the coefficients of the cable model may be reasonably determined within the framework of the linear visco-elasticity.
- (2) It is considered that creep and relaxation of cables tend to increase under influence of prestress. Thus, excessive prestress in comparison with other loads may not be beneficial.

(3) The greater the relative stiffness ratio becomes, the more the creep controls; on the contrary, however, the smaller the ratio becomes, the more the relaxation controls.

(4) At present, the available basic data on the time-dependent behavior of cable-stayed bridges is extremely limited. Thus, further accumulation of the basic data is highly recommended.

### ACKNOWLEDGMENTS

The authors are greatly indebted to Mr. Hiroshi Matsumura of Osaka Municipal Office for his valuable informations and providing the precious data. Furthermore, they are also greatly indebted to all members of Research Committee of Long-Span Steel Bridges of Japanese Construction Consultants Association, Kinki Branch (Chairman : Professor Hiroshi Nakai), for many valuable informations and discussions.

### BIBLIOGRAPHY

- 1) DIN 1073 : Stählenen Strassenbrücken. Berechnungsgrundlagen, 1974.
- 2) Hitachi Zohsen : On creep of Locked Coil Ropes in Onomichi Bridge, Kansai Research Committee on Roadway Bridges, No. B-3, 1977 (in Japanese).
- 3) Osaka Municipal Office : A report on the construction of Kawasaki Bridge, 1979 (in Japanese).
- 4) Kurimoto Steelwork : Measurement on Kawasaki Bridge, 1981 (in Japanese).
- 5) Nakai, M. et al. : Study on creep and relaxation of spiral ropes, Trans. JSME, Vol. 41, No. 343, 1975 (in Japanese), pp.987~993.
- 6) Konishi, I. : Steel bridges, Maruzen, 1976 (in Japanese).
- 7) Metropolitan Highway Authority and Japan Society of Bridge Construction : Research Report on cables for cable-stayed bridges, 1st Report, 1979 (in Japanese).
- 8) Tamura, S. et al. : On design of Onomichi-Ohhashi Bridges, No. 6, 1968 (in Japanese).
- 9) Watanabe, T. et al. : On erection of Onomichi-Ohhashi Bridges, No. 8, 1968 (in Japanese).
- 10) Rabotnov, Y. N. : Creep Problems in Structural Members, Applied Mathematics and Mechanics, Vol. 7, North-Holland Publishing Co., Amsterdam, 1969.
- 11) Lee, E. H. : Stress analysis in visco-elastic bodies, Quart. Appl. Math., Vol. 13, pp.183~190, 1955.
- 12) Sonoda, K., Kobayashi, H. and Ishine, T. : Solutions for beams on linear-elastic foundation, Proc. of JSCE, No. 247, 1976 (in Japanese).
- 13) Yamada, N. and Kunieda, Y. : Laplace transform and operational calculus, Corona Co., 1970 (in Japanese).
- 14) Churchill, R. V. : Operational mathematics, International Student Edition, McGraw-Hill, 1972.
- 15) Kusama, T., Mitsui, Y. and Yoshida, S. : Linear viscoelastic analysis by numerical inversion of the Laplace transform, Proc. of JSCE, No. 292, pp.41~52, 1979 (in Japanese).
- 16) Izumi, Y. : Fundamental study on efficiency of visco-elastic analysis for structures, unpublished M. S. thesis, Kyoto University, 1980 (in Japanese).
- 17) Yamada, I. : Prediction of long-term behavior of cable-stay bridges considering visco-elasticity of cables, Unpublished M. S. Thesis, Kyoto University, 1983.

(Received March 19 1985)